Jordan Journal of Civil Engineering, Volume **8**, No. **3**, **2014**

Effect of Bending Moment Changes on the Rate of Axial Bearing of Composite Columns

Amjad Hameed Abd Al-Razaq

Civil Engineering Department, College of Engineering, University of Kufa, Al-Najaf, Iraq.
E-Mail: amjad881980@yahoo.com

ABSTRACT

At present, Concrete Filled Steel Tubes (CFST) are extensively used in modern structures due to their static and vibrating strength specifications. In this research, a new design model is studied for steel-concrete composite columns under the title of steel tube-shaped columns filled with self-consolidating reinforced concrete with high strength. In this composite column, an I- or cruciform steel hollow-square section is placed inside a square steel tube and the self-consolidating concrete with high strength is poured inside the tube. The ABAQUS software was used to analyze by finite element method (FEM) thirteen composite columns exposed to compression and bending. The effects of the concrete strength, the ratio of width to thickness, the ratio of length to width, and the ratio of the steel cross-section on the strength of these composite columns were evaluated. The results showed that the steel hollow-square section paced inside limited the formation of the diametric shear cracks in the concrete core. Therefore, the failure mode and the post-yield behavior change the composite short columns. The load curves against the axial strain; the stress distribution of the composite columns; and also the interaction curves of the nominal axial load and the nominal bending moment are shown. The comparison of the results computed by the use of FEM modeling showed good compatibility with the laboratory results.

KEYWORDS: Composite columns, Self-consolidating concrete, Steel tube, Shear cracks, Finite-element model, Interaction curves.

INTRODUCTION

Composite columns are a combination of steel and concrete producing a member with useful specifications of the two materials. Steel members enjoy the advantages of ductility and high tensile strength, while concrete members enjoy the advantages of rigidity and high compressive strength. The major advantages of composite columns are their high bearing capacity, ductility and inherent strength (Shams and Saadeghvaziri, 1997; Uy, 2001; Chicoine et al., 2002).

Accepted for Publication on 30/3/2014.

Economic comparison of composite columns with metal columns shows that composite columns consume about 40% to 50% less steel and when compared with concrete columns, composite columns consume about 65% to 80% less concrete, while the consumption of steel is about 10% more (Xi Min et al., 1983). There are two types of major composite systems named steel reinforced concrete columns and concrete-filled tubes. The reinforced concrete-filled steel tube columns with internal steel profile and fibrous concrete effectively increase the resistance against fire (Lie and Kodur, 1996). Also, the steel tube acts like a frame in which the transverse reinforcement in the shape of tie or spirals is omitted. Additionally, the steel tube secures

the continuous confinement to the concrete core. Therefore, the compressive strength and ductility of the concrete is increased. The internal steel profile can definitely improve the fire resistance of these columns compared with CFT columns.

In recent years, the possibility of the use of Self-Consolidating Concrete (SCC) in composite columns has attracted the attention of structure engineers. The self-consolidating concrete shows significant development in concrete technology. This type of concrete can flow and consolidate without vibration in a frame or shuttering under its own weight. The advantages of SCC are the omission of noise, the reduction of construction time, the reduction in vibrating and workshop costs,… etc. Therefore, it can be expected that due to its excellent performance, SCC concrete will be employed in the composite columns in future (Han et al., 2005). On the other hand, the simultaneous presence of axial load and bending moment is something that takes place for a compressive member in most scientific issues. The nominal axial load interaction curve and the column nominal bending moment are the signs of the column failure level at the final bearing instant. The effect of the moment changes on the axial bearing rate of the composite columns is also a new issue on which no extensive research work has been conducted. Therefore, the performance of such a research seems very essential. Therefore, the effect of bending moment changes on the rate of axial bearing of square steel tube columns filled with self-consolidating concrete by the use of numerical and software methods was studied. Of the major goals of this research are:

- The study of the yield post-behavior of the square steel tube column filled with self-consolidating concrete of high strength under the axial load by the utilization of the ABAQUS finite-element method software.
- The study of the effect of concrete strength, ratio of width to thickness and length to different widths on the rate of axial bearing rate of this type of column.
- The determination of the effect of bending moment changes on the rate of axial bearing of composite columns.
- Obtaining the nominal axial load interaction curve and nominal bending moment of the column as the sign for the surface failure of the column at the final bearing instant.

FINITE ELEMENT MODEL

Properties of the Materials

Steel

All the materials employed in the specimens were modeled isotropically. The value of elasticity module was considered to be 2.1x106 kg/ cm^2 and the Poisson ratio was 0.3. The external tube is a cold-formed square tube and the f_{yt} is the yield strength of the tube. The internal steel profile was constructed with the use of a hot-rolled I-shaped beam and the yield strength of the internal profile of f_{ys}. Fig. 1 shows the schematic diagram for the stress-strain relation of the materials in the specimens.

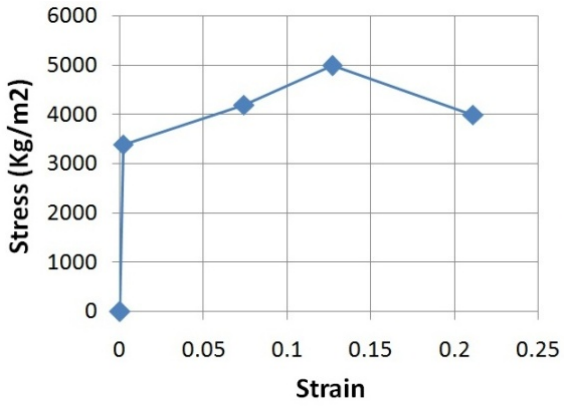

Figure (1): Strain-stress diagram of the consummating steel

Concrete

The damage plasticity model defined in ABAQUS/Standard was used for analysis (Hibbitt et al., 2005). The concrete cubes were cast in 100x100x100 mm and prisms in 150x150x150 mm to determine the compressive strength. The average single-axis

compressive strength of the concrete at low strength was 48.4 MPa and at high strength, it was 708 MPa The elasticity module of the concrete was also 38590 MPa. The strain-stress diagram is shown in Fig. 2.

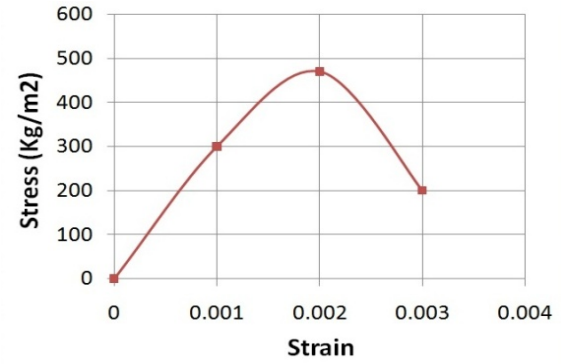

Figure (2): Strain-stress diagram of concrete

The welded steel frame and the specifications of the laboratory specimens are shown in Fig. 3 and Fig. 4, respectively.

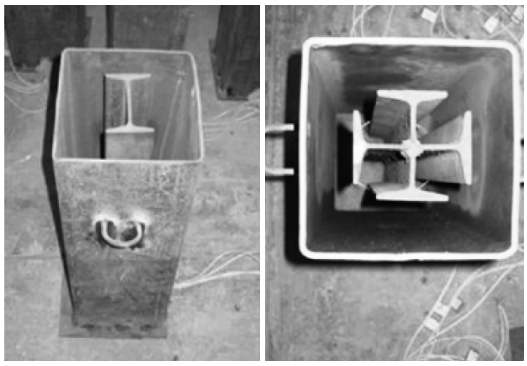

Figure (3): The welded steel frame

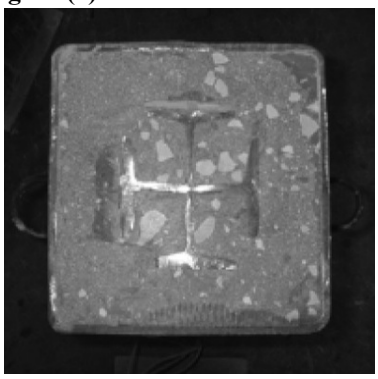

Figure (4): The surface of the specimen before testing

Types of Elements, Mesh Element and Boundary Conditions

The concrete core is modeled with a cubic eight-node element (C3D8R) with 3 degrees of freedom in each group and steel tube as well as internal profile with shell element with 6 degrees of freedom in each node. The shape of the element and the method of meshing of the piece are determined with regard to its geometry and regular meshing is performed in the components individually. The constant boundary conditions are applied on the low levels of the member and the high level of the member is the free boundaries. The compressive concentrated load is applied in the direction of Z downward.

ANALYSIS OF THE MECHANISM

Comparison of the Laboratory Results with the Results Obtained from the ABAQUS Software for Composite Columns under Axial Load

This section is devoted to the responses received, discussion and study of the results of analysis of the finite element of the specimens as well as their comparison with the laboratory results as shown in Figs. 5-8.

Computation of the Final Strength of Square Steel Tube Columns Filled with Self-Consolidating Reinforced Concrete with High Strength

The axial bearing capacity of the square steel tube column filled with self-consolidating reinforced concrete with high strength can be estimated by the following equation:

$$N_0 = A_c f_{cc} + A_t f_{t1} + A_s f_{s1} = \propto A_c f_c + \beta A_t f_{yt} + A_s f_{ys} \quad (1)$$

where,

$$\propto = 1 + 1.2\left(\frac{t}{B}\right)\left(\frac{f_{yt}}{f_c}\right)$$

$$\beta = 1.08 - 0.045 L_n\left(\frac{B}{t}\right)$$

$$f_{t1} = [1.08 - 0.045L_n\left(\frac{B}{t}\right)]f_{yt} \quad (2) \qquad f_{cc} = f_c\left[1 + 1.2\left(\frac{t}{B}\right)\left(\frac{f_{yt}}{f_c}\right)\right] \quad (3)$$

Table 1. Specifications of the laboratory specimens

Name of Sample	B×t×L (mm)	L/B	f'_c (MPa)	A_c (mm^2)	f_{yt} (MPa)	A_t (mm^2)	f_{ys} (MPa)	A_s (mm^2)	ρ_{ss}
S4L	195×4.5×600	3	48.4	34596	289	3429	---	---	0.0
S4H	195×4.5×600	3	70.8	34596	289	4169	---	---	0.0
S4L10	195×4.5×600	3	48.4	31730	289	3429	338	2866	0.083
S4H10	195×4.5×600	3	70.8	31730	289	3429	338	2866	0.083
S5L10	195×5.5×600	3	48.4	30990	288	4169	338	2866	0.085
S5H10	195×5.5×600	3	70.8	30990	288	4169	338	2866	0.085
S4L10I	195×45×600	3	48.4	33163	289	3429	338	1433	0.041
S5L10I	195×5.5×600	3	48.4	32423	289	4169	338	1433	0.042
L4L10-6	195×4.5×1200	6	48.4	31730	289	3429	338	2866	0.083
L4L10-9	195×4.5×1800	9	48.4	31730	289	3429	338	2866	0.083
L4L10-12	195×4.5×2400	12	48.4	31730	289	3429	338	2866	0.083
L5L10I-9	195×5.5×1800	9	48.4	32423	288	4169	338	1433	0.042
L5L10I-12	195×5.5×2400	12	48.4	32423	288	4169	338	1433	0.042

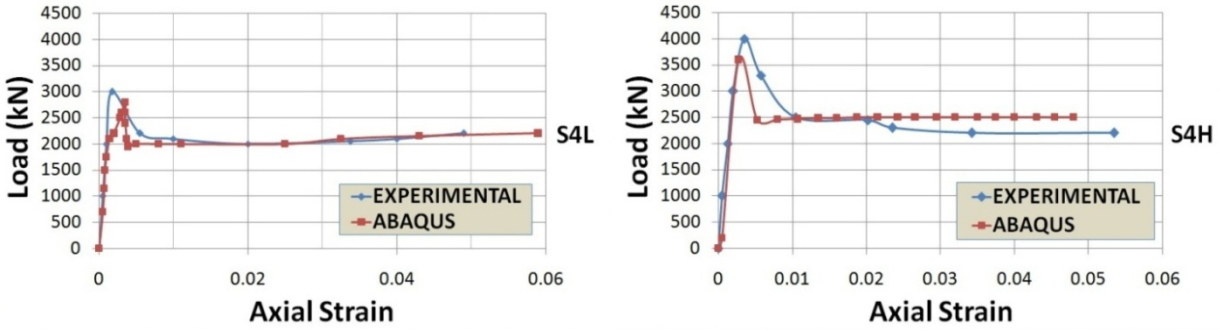

Figure (5): Load curve-the S4L and S4H column axial strain in the ABAQUS software

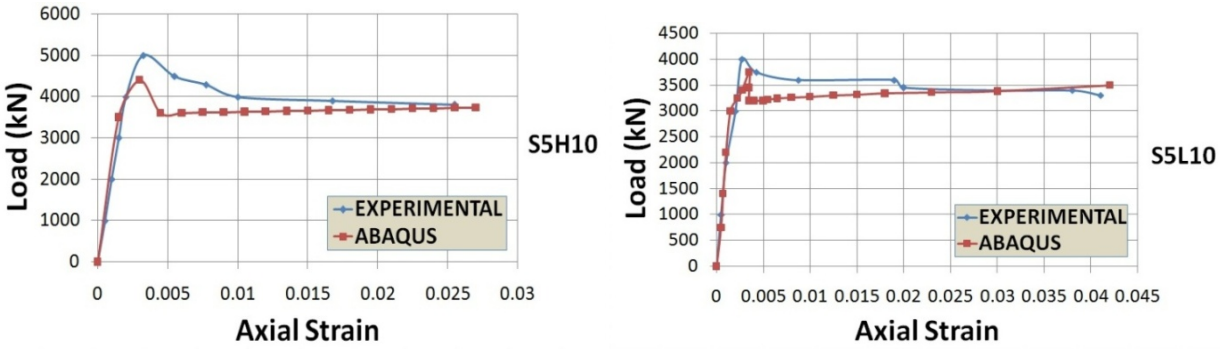

Figure (6): Load curve-the S5H10 and S5L10 column axial strain in the ABAQUS software

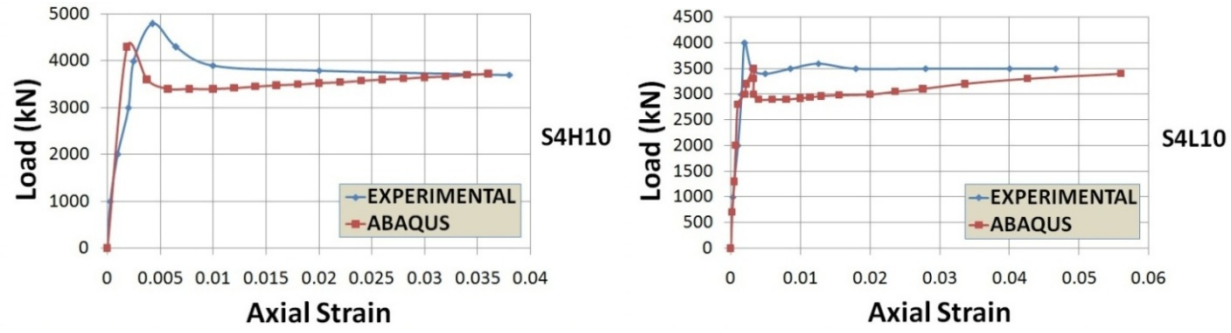

Figure 7. Load curve-the S4L10 and S4H10 column axial strain in the ABAQUS software

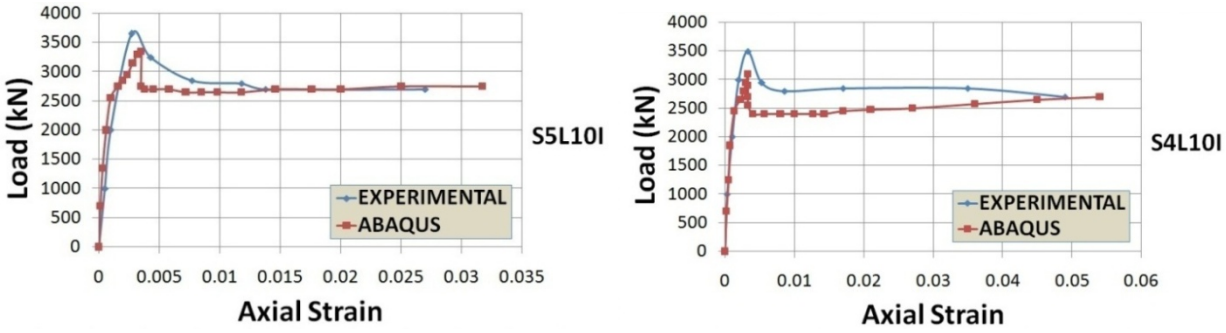

Figure (8): Load curve-the S5L10I and S4L10I column axial strain in the ABAQUS software

In short composite columns under axial compression, the column fails due to the steel yield and cracking of the concrete under direct compression. However, in slender composite columns, the column might yield by elasto-plastic or elastic buckling. When the effect of L/B is considered, the final strength of a composite column under axial compression can be computed by the following equation:

$$N_u = \varphi N_0 \quad (4)$$

Based on design method of the steel-concrete composite members, the φ factor can be computed by the relative slenderness definition of λ for this new type of composite column. According to definition of λ, the following equation can be obtained:

$$\lambda = \frac{L}{\pi}\sqrt{\frac{\alpha A_c f_c + \beta A_t f_{yt} + A_s f_{ys}}{E_c I_c + E_t I_t + E_s I_s}} \quad (5)$$

According to the value of λ, the φ coefficient can be computed by the following equation:

$$\varphi = f(x) = \begin{cases} 1 & \lambda \le 0.2 \\ \frac{1}{2\lambda^2}\left(1 + 0.281\sqrt{\lambda^2 - 0.04} + 4\lambda^2\right. & \\ \left. -\sqrt{(1 + 0.281\sqrt{\lambda^2 - 0.04} + \lambda^2)^2 - 4\lambda^2}\right. & \lambda \ge 0.2 \end{cases} \quad (6)$$

All the obtained loads are summarized in Table 2.

Table 2. Comparison of the axial load capacity of the columns

Name of Sample	Load Capacity (Experimental) (kN) N_u^{exp}	Load Capacity (Nomral) (kN) N_u^{nom}	Load Capacity (Equation) (kN) N_u^{cal}	Load Capacity (Program) (kN) N_u^{abaqus}	$\frac{N_u^{abaqus} - N_u^{exp}}{N_u^{exp}}$	$\frac{N_u^{exp}}{N_u^{nom}}$	$\frac{N_u^{exp}}{N_u^{cal}}$
S4L	2985	2665	2856	2751	-8%	1.12	1.045
S4H	3900	3440	3631	3531	-9%	1.13	1.074
S4L10	3930	3495	3663	3531	-10%	1.12	1.073
S4H10	4750	4206	4374	3664	-8%	1.13	1.086
S5L10	4050	3669	3879	3768	-7%	1.10	1.040
S5H10	4880	4363	4573	4372	-10%	1.12	1.067
S4L10I	3410	3080	3259	3104	-9%	1.11	1.046
S5L10I	3620	3254	3478	3344	-7.5%	1.11	1.041
L4L10-6	3765	3495	3496	3452	-8%	1.08	1.077
L4L10-9	3720	3495	3312	3411	-8.3%	1.06	1.123
L4L10-12	3410	3495	3130	3079	-10%	0.98	1.089
L5L10I-9	3520	3254	3171	3147	-10.5%	1.08	1.110
L5L10I-12	3245	3254	3010	2946	-9%	1.00	1.078

The Study of the Interaction Curves of the Axial Bending Moment Load

In this section, three tube-shaped short columns filled with concrete without internal profile and with internal I-shaped profile (S4L, S4L10I, S5L10I), two short tube-shaped columns filled with concrete with cruciform internal profile (S4L10, S5L10), three tube-shaped short columns filled with concrete with high strength (S4H, S4H10, S5H10), two slender columns with I-shaped internal profile (L5L10I-9, L5L101-12) and three slender columns with cruciform internal profile (L4L10-6, L4L10-9, L4L10-12) were placed under an axial load with different eccentricities (1e, 3e, 5e, …) and analyzed. The values of the axial load were obtained from each analysis and by multiplying them by the related eccentricity, the nominal bending moment was obtained. The first point observed in the study of S4L10, S5L10S4L, S4L10I and S5L10I diagrams is the very decreasing trend of axial capacity drop due to an increase in eccentricity (from 0 to 23e) which is clearly observed. This trend of decrease up to the eccentricity of e=3cm reveals less drop indicating the continuity between the steel tube, concrete and the internal profile after obtaining the final load and securing continuous confinement of the concrete by the steel tube. In this manner, after the eccentricity of e=3cm, this axial capacity drop takes place with greater intensity and 3e=9cm point is considered as a boundary state between compressive failure and tensile failure. In S4H10, S5H10 and S4H contrary to the specimens with less strength, the reduction trend shows more drop by an increase in the eccentricity of e=3cm, while 5e=15cm point is considered as a boundary state between compressive failure and tensile failure. In L5L10I-9, L5L10I-12, L4L10-6, L4L10-9 and L4L10-12 specimens, the trend of reduction shows more drop by an increase in the eccentricity of e=4cm and 5e=20cm point is considered as a boundary state between compressive failure and tensile failure. Figs. 9-13 show diagrams with bending moment-axial load.

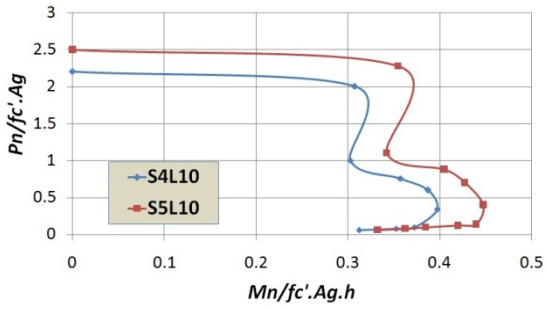

Figure (9): Diagrams of the bending moment-axial load of S4L10 and S5LI0 columns

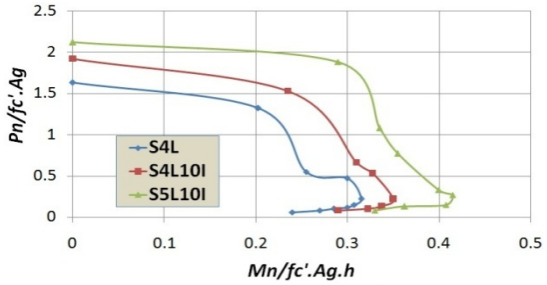

Figure (10): Diagrams of the bending moment-axial load of S4L, S4L10I and S5L10I columns

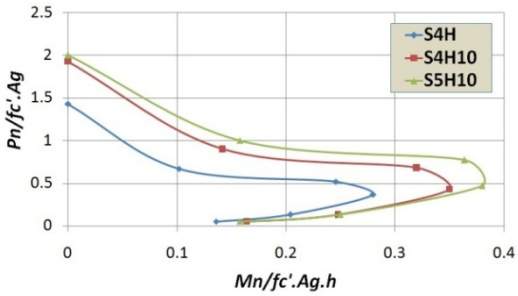

Figure (11): Diagrams of the bending moment-axial load of S4H, S4H10 and S5H10 columns

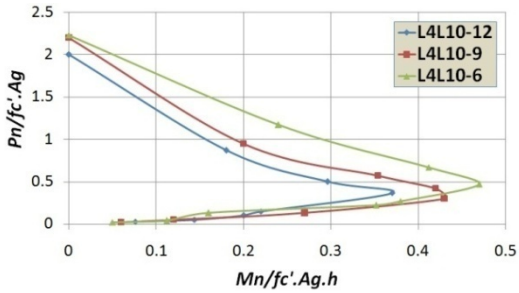

Figure (12): Diagrams of the bending moment-axial load of L4L10-6, L4L10-9 and L4L10-12 columns

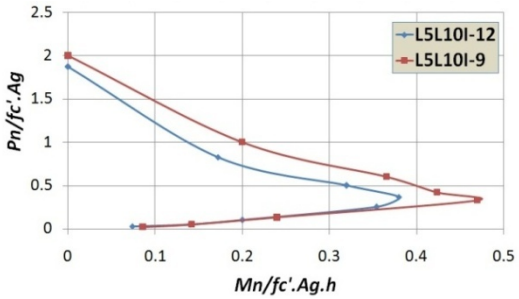

Figure (13): Diagrams of the bending moment – axial load of L5L10I-9 and L5L10I-12 columns

CONCLUSIONS

1. The failure modes of composite columns with and without internal steel profile (S4H and S4H10) are completely different; since the steel profile can effectively delay or limit the occurrence of slippage shear cracks in the concrete with high strength. Therefore, it changes the response after the peak point of the composite short columns.
2. In composite short columns with cruciform internal profile, the stress location is observed at maximum in the middle of the height and in the web of the profile, but in columns with I-shaped internal profile, it is observed in the middle of the height and in the flange of the profile and with an increase in the thickness of the steel tube, the values of these stresses are reduced.
3. In composite slender columns, the location of stress is observed at maximum in the low section, near the fixed edge and in the internal profile flange.
4. The axial compressive-strain load curve of short columns before a load of about 80% of final strength approaches the linear state. After this load level, the steel starts yielding and the load curve is deviated from the initial linear state. The response after the peak point of the columns is under the effect of f_c', B/t and ρ_{ss}.
5. The compressive strength of the column is reduced by an increase in the L/B ratio due to the failure resulting from instability and an increase in the lateral deformations. Therefore, the composite column with a large L/B ratio is not suggested for engineering work.
6. In the study of the bending moment (dimensionless)and compressive load interactive curves, the decreasing trend of the axial capacity drop due to the effect of an increase in eccentricity is clearly observed, but in short columns, this decreasing trend shows less drop up to the eccentricity of e=3 cm and after that it continues with more drop.
7. The rate of axial capacity drop up to e=3 cm

eccentricity in short composite columns with cruciform internal profile is less relative to composite columns with I-shaped internal profile.

8. In the study of the interactive curves of compressive load and bending moment (dimensionless), slender columns show that by an increase in eccentricity, the axial capacity is greatly dropped and by an increase in the slenderness of the columns, the bearing capacity is reduced.
9. In short columns, the point 3e= 9 cm (e=3 cm) is considered as a boundary between tensile failure and compressive failure. The interactive diagram is in a reversible state at this point.
10. In slender columns, the interactive diagram is in a reversible state at 5e= 20 cm (e=4 cm) and this point is considered as the boundary between tensile failure and compressive failure.

NOMENCLATURE

A_c = The concrete cross-section area = m^2
A_t = The cross-section of the tube = m^2
A_s = The profile cross-section area = m^2
B = Width of the column = mm
CFST = Concrete Filled Steel Tubes
CFT = Fire resistance of these columns
C3D8R = Cubic eight-node element
E_c= Concrete elasticity module = mm^2
E_s= Steel profile elasticity module= mm^2
E_t = Steel tube elasticity module = mm^2
e = Eccentricity
FEM = Finite element method
f_{cc} = Confined concrete strength = MPa
f_n = Axial stress of square steel tube in the final load = MPa
f_{s1} = f_{sy} of the axial stress of the steel profile in the final load = MPa
f_{ys} = Yield strength of the internal profile= MPa
I_c = Concrete inertia moment = mm^4
I_t = Steel tube inertia moment = mm^4
I_s = Steel profile inertia moment = mm^4
L = Effective length of the composite column = mm
N_0= Final strength of square steel tube columns filled with self-consolidating reinforced concrete with high strength = kN
SCC = Self-consolidating concrete.
φ = Reduction factor due to the slenderness of the column = dimensionless

REFERENCES

Chicoine, T., Tremblay, R., Massicotte, B., Ricles, J. M., and Lu, L. W. (2002). "Behavior and strength of partially encased composite columns with built-up shapes". J. Struct. Eng., ASCE, 128 (3), 279-287.

Han, L. H., Yao, G. H., and Zhao, X. L. (2005). "Tests and calculations for hollow structural steel (HSS) stub columns filled with self-consolidating concrete (SCC)". J. Constr. Steel Res., 61 (9), 1241-1269.

Hibbitt, Karlson and Sorensen, Inc. (2003). "ABAQUS standard users manual. version 6.4.1". Hibbitt, Karlsson and Sorensen, Inc.

Kodur, V. K. R. (1999). "Performance–based fire resistance design of concrete –filled steel columns". J. Constr. Steel Res., 51, 21-36.

Kodur, V. K. R., and Lie, T.T. (1996). "Fire resistance of circular steel columns filled with fiber-reinforced concrete". J. Struct. Eng., ASCE, 122 (7), 776-782.

Lie, T. T., and Kodur, V. K. R. (1996). "Fire resistance of steel columns filled with bar-reinforced concrete". J. Struct. Eng., ASCE, 122 (1), 30-36.

Shams, M., and Saadeghvaziri, M. S. (1997). "State of the art of concrete-filled steel tubular columns". ACI Struct. J., 94 (5), 558-571.

Uy, B. (2001). "Local and post-local buckling of fabricated thin walled steel and steel-concrete composite sections". J. Struct. Eng., ASCE, 127 (6), 666-677.

Xi, Min, Shen, Guanzao Tang and Bingguan Zhao. (1983). "Building with concrete-filled steel columns". Batiment International Building Research and Practice, 11 (5), 311-316.